C1orf61 promotes hepatocellular carcinoma metastasis and affects the therapeutic response to sorafenib

You Yu
Wuhan University
Zhimeng Wang
Wuhan University
Zan Huang
Wuhan University
Xianying Tang
South-Central University for Nationalities
Wenhua Li (whli@whu.edu.cn)
Wuhan University

Research

Keywords: C1orf61, HCC, Metastasis, Sorafenib treatment

Posted Date: September 24th, 2020

DOI: https://doi.org/10.21203/rs.3.rs-80702/v1

Abstract

Background

C1orf61 is a specific transcriptional activator that is highly up-regulated during weeks 4–9 of human embryogenesis, the period in which most organs develop. We have previously demonstrated that C1orf61 acts as a tumor activator in human hepatocellular carcinoma (HCC) tumorigenesis and metastasis. However, the underlying molecular mechanisms of tumor initiation and progression in HCC remain obscure.

Methods

In this study, we demonstrated that the pattern of C1orf61 expression was closely correlated with metastasis in liver cancer cells. Gene expression profiling analysis indicated that C1orf61 regulated diverse genes related to cell growth, migration, invasion and epithelial-mesenchymal transition (EMT).

Results

Results showed that C1orf61 promotes hepatocellular carcinoma metastasis by inducing cellular EMT in vivo and in vitro. Moreover, C1orf61-induced cellular EMT and migration are involved in the activation of the STAT3 and Akt cascade pathways. We also found that C1orf61 was associated with HBV infection-induced cell migration in HCC. In addition, C1orf61 expression improved the efficacy of the anticancer therapy sorafenib in HCC patients. For the first time, we report a regulatory pathway by which C1orf61 promoted cancer cell metastasis and regulated the therapeutic response to sorafenib.

Conclusions

These findings increased our understanding of the molecular events that regulate metastasis and treatment in HCC.

Background

Hepatocellular carcinoma (HCC) is one of the most lethal cancers. Worldwide, HCC results in approximately 600,000 deaths each year. [1, 2] Infiltration into adjacent tissues and metastasis to distant organs are the causes of death in the majority of HCC patients. [3, 4] Thus far, the detailed molecular mechanisms underlying the initiation and progression of tumor metastasis remain far from fully understood. As a result, medical prevention and treatment of HCC is disappointing.

HCC metastasis occurs via multiple steps, including neoangiogenesis, local invasion, intravasation, extravasation, and the colonization of a secondary anatomical site. [5] Many genes encoding cell surface

receptors and secretory proteins cooperate are involved in a complex molecular network as part of this process. Some well-known components, such as metalloproteinase (MMPs), [6] Wnt, [7] transforming growth factor beta (TGF-β), [8] vascular endothelial growth factor (VEGF), [9] fibroblast growth factor (FGF) [10] and platelet-derived growth factor (PDGF), [11] play important and heterogeneous roles in cell survival, growth, proliferation, epithelial-mesenchymal transition (EMT) and metastasis. [12–14] Stromal components, including fibroblasts, vascular endothelia cells, nerve cells, inflammatory immune cells, mesenchymal stem cells (MSCs) and the surrounding extracellular matrix (ECM), play synergetic roles in maintaining tumor microenvironments. [15] This is an essential driver of HCC initiation, progression, invasion, and metastasis. [16] Some oncogenes may also play a more global role in regulating tumor metastasis. For example, gene expression signatures derived through transcriptional profiling indicated that the transcription factor MYC is specifically necessary for invasion and metastasis; MYC regulates downstream programs to regulate the expression of relevant genes or affects cancer cell EMT. [17]

C1orf61 (chromosome 1 open reading frame 61) is a specific transcriptional activator of c-fos that is widely expressed in proliferating and migrating cells of the developing brain. [18] We have previously demonstrated using gene expression profiling that C1orf61 is highly up-regulated during weeks 4–9 of human embryogenesis, the critical period when most organs develop. [19] However, potential regulatory mechanisms and the mode of action of C1orf61 in inducing human liver cancer cell metastasis remains obscure.

In this study, we investigated the functions of C1orf61 in hepatocellular carcinoma metastasis. Our data showed that the level of C1orf61 expression was correlated with metastasis in liver cancer cells. C1orf61 promoted human hepatocellular cell invasion and migration in vitro and in vivo. In this process, C1orf61 activated STAT3 and Akt cascade pathways. In turn, these pathways promoted liver cancer cells towards EMT and eventually resulted in metastasis. Moreover, C1orf61 affected the response of liver cancer cells to sorafenib therapy. In this study, we present a novel mechanism by which C1orf61 contributes to metastasis in HCC. Our findings identify C1orf61 as a new candidate for use in diagnosis, prognosis, and targeted therapy in HCC patients.

Materials And Methods

Cell lines and cell culture

The following human liver cancer cell lines were used: (a) SMCC7721 and Hep3B cells were kindly provided by Dr. Zhiyong Mao (Tongji University), (b) HCCLM9 cells were obtained from the Wuhan University School of Medicine, (c) HepG2, HepG2.2.15, BEL7402, Huh7, FHCC98, and the immortalized non-malignant human normal liver cell line L02 were stored in our lab and (e) the stably transfected cell lines L02-C1orf61, BEL7402-C1orf61, HCCLM9 sh-C1orf61, Huh7 sh-C1orf61 were established by our lab. HCCLM9 C1orf61-/- cell lines were established in our lab using the CRISPR/Cas system. Cells were all cultured in DMEM supplemented with 10% fetal bovine serum, penicillin (1000 U/ml), and streptomycin

(1000 μg/ml) in a humidified chamber with 5% CO_2. Cell culture dishes and plates were obtained from Wuxi NEST Biotechnology Co. Ltd. (Wuxi, China).

Microarrays and qRT-PCR

Total RNA was isolated using TRIzol reagent (Life technologies, Carlsbad, CA, US) according to the manufacturer's instructions. Samples were purified using the RNeasy Mini Kit (Qiagen, GmBH, Germany). RNA samples from each group were then used to generate biotinylated cDNA targets for use in an Affymetrix GeneChip® Human Transcriptome Array 2.0. The biotinylated cDNA targets were then hybridized to the microarray. After hybridization, arrays were stained in a Fluidics Station 450 and scanned on an Affymetrix Scanner3000. The microarray experiments were performed following the protocol described by Affymetrix Inc. at Shanghai Biotechnology Corporation. The raw data were normalized using the SST-RMA method by an Expression console (Affymetrix). Ratios were calculated between L02-PHAGE, L02-C1orf61 and Huh7 cells. Genes with fold changes of at least 2 were selected for further analysis.

Plasmids and transfection

Two empty vectors, pHAGE.puro and PLKO.1.Sunny, were kindly provided by Dr. Zan Huang (Wuhan University). The empty vectors p-USE and p-USE-CA-Akt plasmids were purchased from Upstate Biotechnology (Lake Placid, NY, USA). shRNA targeting C1orf61 were purchased from GENECHEM Biotechnology (Shanghai, China). Cells were seeded in six-well plates, and plasmids were transfected for 48 hours with PEI (provided by Dr. Xiaodong Zhang).

Soft agar colony formation assay

BEL7402-PHAGE-puro cells (5×10^3/ml) or BEL7402-C1orf61-puro cells (5×10^3/ml) were suspended in the top layer of 0.6% agar, which was then laid on a bottom layer of 1.2% agar. Cells were incubated in soft agar plates at 37 °C for 14–20 days. Colonies were photographed and quantified.

Western Blot analysis and ELISA

After each treatment, cells were lysed and proteins were collected and their expressions were assessed by Western blot as previously described. Antibodies against C1orf61 was purchased from GL Biochem Ltd (Shanghai, China); the E-cadherin, N-cadherin, Vimentin, Occludin, Snail, p-Akt, Akt, STAT3, Caspase3, PARP antibodies were purchased from Cell Signaling Technology (Beverly, MA); the p-STAT3 (Y705F) antibody was purchased from Santa Cruz Biotechnology (Santa Cruz, CA); and the β-actin, GAPDH antibodies were purchased from ProteinTech Group Inc (Chicago, IL, USA).

The levels of HBs and HBe in cultured supernatants were measured by ELISA to identify the transfection efficiency, following the instructions of Beyotime.

Immunofluorescence (IF)

Briefly, cells were seeded on coverslips and fixed with 4% paraformaldehyde for 20 minutes at room temperature. Cells were then washed twice with PBS and incubated with primary antibodies against E-cadherin, Vimentin, p-STAT3 (Y705F) at 4 °C overnight. After thorough washing, the cells were incubated with fluorescence-conjugated secondary antibodies for 1 h. Nucleus were stained with DAPI (Beyotime). Fluorescent images were visualized using a confocal laser-scanning microscope (Fluoview FV1000; Olympus, Tokyo, Japan).

Wound-healing assay

Cellular migration was determined by a scratch wound healing assay. Cells were seeded into a six-well plate and were allowed to reach confluence. A wound was created by scraping the monolayer of the well with a 200 μl pipette tip. The fresh complete medium was added after the floating cells were carefully removed. The cells were incubated at 37 °C for 24 h or 36 h. Images of the wound area was captured in three fields using an inverted light microscope (Olmpus).

Transwell assay

Cellular migration was performed in a 24-well Transwell Assay Chamber (PET track-etched membrane; Becton Dickinson, Franklin Lakes, NJ, USA). Cells in serum-free medium were seeded into the top chamber, whereas complete medium with or without S3I-201 (50 μM) or LY294002 (10 μM) was added to the bottom chamber. After incubation for 24 h or 36 h at 37 °C, non-migrated cells on the top side of the membrane were removed and cells on the bottom side were fixed and stained with 0.5% crystal violet for 20 min. Quantification of the migrated cells were done by counting nine random fields under the microscope.

Luciferase Reporter Assay

Cells were seeded at approximately 60% confluence in 24-well plates. 0.2 μg Akt luciferase reporters were transfected into L02-PHAGE, L02-C1orf61, HCCLM9 WT, and HCCLM9 sh-C1orf61 cells using PEI. The pRL-TK plasmid was used as an internal transfection control. After 36 hours, firefly and Renilla luciferase activities were measured.

Cell proliferation and cell viability assays

Sorafenib was dissolved in DMSO before use. The effect of sorafenib on cell proliferation was characterized by cell counting. Cells were seeded at a density of 3×10^3 in a 96-well plate and cultured for 48 hours after treatment with the indicated doses of sorafenib. The cells were counted using a hemocytometer. Cell viability was measured using a trypan blue dye staining assay.

In vitro apoptosis assay

For the apoptosis assay, treated cells were harvested by 0.05% EDTA-trypsin, then washed with PBS, resuspended in 1 × binding buffer and stained with Annexin V-FITC and propidium iodide (PI) for 15 min at room temperature. Annexin V-FITC and PI fluorescence were measured with a flow cytometer (Beckman-Counter).

Tumour xenograft assay

Five-week-old male BALB/C nude mice were purchased from the Model Animal Research Center (Changsha, China). Animals were handed according to the guidelines of the Laboratory Animal Center of Wuhan University. All experiments were conducted under approved procedures. HCCLM9 WT, HCCLM9 C1orf61-/- #1, HCCLM9 C1orf61-/- #2 cells were resuspend in 0.2 ml PBS and 5×10^6 cells were injected in the right flank or 1×10^6 cells were injected into tali vain. For flank tumor injection, tumor volumes and body weights were measured and recorded everyday. Tumor volumes were calculated as length × width^2/2.

Tissue protein isolation and immunohistochemistry (IHC)

For flank tumor injection, mice were kept for 5 weeks and then sacrificed. For tail intravenous injection, mice were kept for 50 days and then sacrificed. Tumor tissues were extracted and washed in PBS and then stored at -80 °C. For western blot assay, the tumor tissue was lysed in RIPA buffer on ice and then centrifuged at 12000 g for 15 min at 4 °C to collect the supernate, and the proteins were subjected to Western bolt analysis, as described previously.

Lungs were harvested and immediately fixed in 4% paraformaldehyde solution and subsequently paraffin embedded, sectioned and stained with H and E. Tumor tissues were fixed in 4% paraformaldehyde solution and embedded in paraffin and sectioned (5 μm) for immunohistochemistry. The sections were incubated with the primary antibodies (E-cadherin, Vimetin, p-STAT3, p-Akt/Akt antibodies). The sections were further incubated with biotinylated goat anti-rabbit and goat anti-mouse antibodies. The specific signals were then detected with streptavidin-conjugated horseradish peroxidase and with the use of diaminobenzidine as the chromogen.

Statistical analyses

Student's t test was used for statistical analyses. All data were expressed as the means ± SD. $P < 0.05$ was considered statistically significant.

Results

Expression of C1orf61 promotes human liver cancer cell migration

To evaluate the effect of C1orf61 on cancer cell metastasis, we first examined the relationship between the expression level of C1orf61 and HCC migration. Wound-healing assays and transwell assays showed that the expression level of C1orf61 positively correlated with cell migration in human liver cancer cells. HCCLM9 cells that expressed the highest level of C1orf61 possessed the strongest migration ability compared to other cell lines (Fig. 1a and Fig. S1a, b). Furthermore, we found that the up-regulation of C1orf61 promoted migration in BEL7402 and L02 cells; in contrast, C1orf61 knock-down inhibited

migration in HCCLM9 and Huh7 cells (Fig. 1b, c and Fig. S1c, d). Similarly, knock-out of C1orf61 using CRISPR/Cas9 also significantly inhibited cell migration in HCCLM9 cells (Fig. 1d and Fig. S1e, f). Anoikis and soft agar colony formation suggested that multicellular survival and anchorage-independent growth occurred when cells were removed from inappropriate cell/ECM interactions; [20] these abilities were closely related to the metastasis potential of cells. Figure 1e and f show that C1orf61 expression inhibited anoikis in cells and promoted anchorage-independent growth without correct attachment in HCC. Taken together, these data suggest that the intracellular level of C1orf61 was associated with metastatic potential and the high expression of C1orf61 promoted cellular migration in human liver cancer cells.

C1orf61 regulates EMT-related gene expression and induces cellular EMT

To investigate the underlying molecular signaling events involved in C1orf61-mediated cell migration, we first performed gene expression profiling analysis using L02 (low C1orf61 expression), L02-C1orf61 (C1orf61 overexpression) and Huh7 cells (high C1orf61 expression). The results showed that C1orf61 regulated the expression of a diverse set of genes associated with biological function, cellular components and molecular activity (Fig. 2a and Fig. S2a). Further comparison and analysis revealed that some genes were related to cell growth, migration, invasion and EMT (Fig. 2b). RT-PCR results for a number of genes were all consistent with the microarray data, suggesting that the gene expression profiling array was correct (Fig. 2c). EMT is a key process in the metastatic cascade in tumors. It is regulated by multiple genes and complex interactions within the tumor microenvironment. Next, we examined whether C1orf61-induced cell migration was associated with EMT. Microscopy showed that the morphology of highly expressed C1orf61 cells changed from tightly packed colonies into spindle-shaped cells; the latter morphology is a typical feature of cells undergoing EMT (Fig. 2d). Moreover, isothiocyanate-conjugated phalloidin staining indicated that C1orf61 expression promoted BEL7402 and HCCLM9 cells to reorganize F-actin into parallel bundles and form lamellipodia. These findings were consistent with the cellular morphology results (Fig. 2e). To further confirm above observation, we examined the status of epithelial and mesenchymal cell markers by Western blotting and immunofluorescence analyses. As shown in Fig. 2f and Fig. S2b, overexpression of C1orf61 in L02 and BEL7402 cells resulted in a decrease in the protein levels of the epithelial cell markers E-cadherin and occludin and the up-regulation of the mesenchymal cell markers N-cadherin, Vimentin and Snail. Correspondingly, C1orf61 knock-down in HCCLM9 and Huh7 cells resulted in a decrease in the protein levels of the mesenchymal cell markers and increased epithelial cell markers (Fig. 2f and Fig. S2b). Similar results were observed when C1orf61 was knocked-out in HCCLM9 (Fig. S2c, d). Therefore, we propose that C1orf61-induced cell migration is associated with the promotion of EMT in human liver cells.

Activating STAT3 is essential for C1orf61-induced cellular EMT and migration

Signal transducer and activator of transcription 3 (STAT3) is a transcription factor involved in a major cascade responsive to stimulation by many growth factors and cytokines. [21] STAT3 is involved in the

regulation of cell proliferation, apoptosis, cell invasion, angiogenesis and EMT processes. [22–24] Hence, we determined the levels of STAT3 and phosphorylated-STAT3. As shown in Fig. 3a, cells with high levels of C1orf61 protein expressed high levels of the phosphorylated-STAT3. These proteins were also translocated into the nucleus, where STAT3 regulates the expression of other genes (Fig. 3b and Fig. S3a). The STAT3-specific inhibitor S3I-201 suppressed endogenous STAT3 phosphorylation and blocked the transfer of STAT3 into the nucleus (Fig. S3b). Correspondingly, the suppression of STAT3 with S3I-201 also impaired EMT in cells and attenuated cell migration in L02-C1orf61 but not L02 cells (Fig. 3c, d and Fig. S3c, d). Ectopic expression of STAT3 in L02 cells increased the STAT3 protein level and facilitated the transfer of STAT3 into the nucleus as expected (Fig. S3e). In this scenario, the protein levels of epithelial cell markers (E-cadherin and Occludin) were reduced and mesenchymal cell markers (N-cadherin, Vimentin) were up-regulated; cell migration was also promoted (Fig. 3e, f and Fig. S3f, g). The overexpression of STAT3-Y705F, which is an artificially generated STAT3 containing a point mutation in tyrosine 705 resulting in a phenylalanine substitution, resulted in a pronounced dominant-negative effect on the activation of wild-type STAT3. STAT3-Y705F overexpression also inhibited cellular EMT and prevented migration (Fig. 3e, f and Fig. S3f, g). These results suggested that the activation of STAT3 has a significant promoting effect on C1orf61-induced cellular EMT and migration.

Akt activation is also involved in C1orf61-induced cellular EMT and migration

It has been shown that Akt is a key mediator of tumor metastasis and EMT induction in the progression of many human tumors. [25, 26] Next, we evaluated the role of Akt in C1orf61-mediated cellular EMT and migration. As shown in Fig. 4a, ectopic C1orf61 expression in L02 and BEL7402 cells remarkably increased the level of phosphorylated Akt. C1orf61 silencing in HCCLM9 and Huh7 cells robustly suppressed Akt phosphorylation. A luciferase assay reflecting PI3K/Akt pathway activation also confirmed that high C1orf61 expression significantly enhanced the PI3K/Akt activity (Fig. 4b). This finding was consistent with the phosphorylation level. To examine whether Akt activation plays a role in C1orf61-induced cellular EMT and migration, we treated cells with the specific PI3K/Akt inhibitor LY294002. The results showed that Akt inactivation by LY294002 increased E-cadherin expression and suppressed the level of N-cadherin in L02-C1orf61 cells. Moreover, wound-healing and transwell assays indicated that LY294002 significantly decreased cell migration in L02-C1orf61 cells; cell migration did not decrease in L02 cells where C1orf61 expression was low (Fig. 4c, d and Fig. S4a, b). In contrast, the ectopic expression of continually activated Akt (Akt CA) induced EMT in L02 cells and facilitated migration; the migration ability of these cells approached that of L02-C1orf61 cells (Fig. 4e, f and Fig. S4c, d). These results revealed that Akt was involved in C1orf61-induced cellular EMT and migration.

C1orf61 Promoted Tumor Growth And Facilitated Metastasis In Vivo

To evaluate the effects of C1orf61 on tumor growth and metastasis in vivo, we established subcutaneous tumor xenograft models and an experimental metastasis assay (intravenous tumor cell inoculation) in

athymic nude mice using HCCLM9 wild type and HCCLM9 C1orf61 knock-out cells, respectively. As shown in Fig. 5a and b, subcutaneous tumors containing HCCLM9 wild type cells grew dramatically faster than those containing C1orf61 knock-out cells after 28 days later. This was reflected in both tumor volume and weight. These observations revealed that C1orf61 facilitated tumor growth in vivo. To determine whether C1orf61 knock-out in HCCLM9 cells modulated the development of metastasis, we examined the formation of lung metastases in subcutaneous and intravenous tumor models. As shown in Fig. 5c and d, C1orf61 knock-out resulted in a significant reduction in metastatic animals and decreases in the number of metastatic nodules in the lung. Further examination of the expression of some related proteins by Western blot and immunohistochemistry indicated that C1orf61 knock-out inhibited cellular EMT, decreased STAT3 and Akt activity; in vivo results were consistent with in vitro findings (Fig. 5e and f). These data suggested that the up-regulation of C1orf61 promoted tumor growth and metastasis in vivo. The potential molecular mechanism may be related to the induction of cellar EMT, STAT3 and Akt regulation.

C1orf61 is involved in HBV infection-induced cell migration in HCC

Hepatitis B virus (HBV) is a major etiological factor for HCC and is closely associated with regulating liver cell malignancy, proliferation, metastasis and apoptosis. [27, 28] Here, we determined whether C1orf61 modulated HBV infection-induced cell migration. HepG2.2.15 is a liver cancer cell line integrated with HBV; these cells exhibited increased EMT and migration compared to HepG2 cells without HBV infection. However, C1orf61 knock-down remarkably impaired HBV infection-induced cell migration (Fig. 6a, b and Fig. S5a). To further confirm the role of C1orf61 in HBV-induced cell migration, L02-PHAGE cells were infected with HBV; EMT and migration potential were then examined. As shown in Fig. 6c and Fig. S5b, c, C1orf61 levels were positively correlation with HBV infection-induced EMT and migration. These findings were consistent with that of HepG2 cells. The HBV genome encodes some primary proteins associated with infection and virus replication. These proteins include HBe, HBs, HBc, HBp and HBx, which regulate multiple HCC processes. Next, we determined which elements play critical roles in C1orf61-mediated tumor metastasis. Real-time PCR and Western blot analyses indicated that the transient expression of HBe and HBc remarkably increased C1orf61 mRNA and protein levels (Fig. 6d). Importantly, HBe and HBc induced C1orf61 expression in a transfection dose-dependent manner and facilitated EMT (Fig. 6e). Further wound-healing and transwell assays revealed that C1orf61-knockdown inhibited cell migration by HBe and HBc (Fig. 6f and Fig. S5d,e). These results showed that HBV, particularly the HBe and HBc proteins, promoted the migration of HCC cells via the up-regulation of C1orf61 expression.

C1orf61 improves the therapeutic response to sorafenib in HCC cells

Sorafenib, an oral small molecule multikinase inhibitor, has been recently approved for the treatment of hepatocellular carcinoma. Functionally, sorafenib inhibits tumor growth and angiogenesis, induces apoptosis and remodels the tumor microenvironment. [29, 30] We next examined whether C1orf61 regulated cancer treatment in HCC. As shown in Fig. 7a and Fig. S6a, HCCLM9 cells highly expressing C1orf61 exhibited a more sensitive response to sorafenib treatment than other cells lines in regard to cell

proliferation inhibition and induced cell death. BEL7402 cells, which express C1orf61 at a low level, showed relative resistance. We speculated that C1orf61 was involved in the regulation of sorafenib treatment. To further confirm this hypothesis, the same dose of sorafenib was used to treat BEL7402-PHAGE and BEL7402-C1orf61 or HCCLM9 and HCCLM9 C1orf61-/- cells. The results indicated that cells highly expressing C1orf61 performed better in response to sorafenib treatment (Fig. 7b). FACS and Western blot analyses of apoptosis revealed that the capacity of sorafenib to induce apoptosis was closely related the expression level of C1orf61 in human liver cells (Fig. 7c and Fig. S6b). Moreover, we also found that 4 μM sorafenib inhibited migration and repressed EMT in cells with a high level of C1orf61 but not in cells with low level of C1orf61 (Fig. 7d, e and Fig. S6c, d). Altogether, these findings strongly suggest that C1orf61 improved the efficacy of sorafenib anticancer therapy against HCC.

Discussion

C1orf61 is located at human chromosome 1, band q22. Gene amplification in this region is enriched in hepatocellular carcinoma. Gene expression profiling revealed that this gene is highly expressed during weeks 7–9 of human embryogenesis in particular. [18, 19] Numerous developmental genes have been reported as associated with tumor progression and treatment. [31] Recent studies have demonstrated that C1orf61 is overexpressed in a population of liver cancer stem cells characterized by the expression of the membrane protein $CD133^{+}$. We have previously reported that C1orf61 is widely expressed in both proliferating and migrating cells during brain and bone development. Taken together, these findings implied that C1orf61 plays a critical role in the initiation and progression of hepatocellular carcinoma. Tumor metastasis is a clinical challenge that is the causative agent of the majority of cancer patient deaths. Although our understanding of the molecular events that regulate metastasis has universally improved, the processes of metastasis associated with C1orf61 remain unknown. The data presented here demonstrate that C1orf61 promoted human hepatocellular cell metastasis. In turn, the downstream of transcription factors STAT3 and Akt kinase are activated. This eventually induces EMT and cell migration. Moreover, C1orf61 is involved in regulating HBV infection-induced cell migration and affects therapeutic response to sorafenib in HCC cells (Fig. 7f).

In human hepatocellular carcinoma, C1orf61 exhibited controversial functions in tumor progression and cancer treatment. C1orf61 facilitated liver cancer initiation and metastasis, revealing a role in pro-oncogene activation and posing risk to healthy people when abnormally highly expressed. Conversely, C1orf61 improved the efficacy of sorafenib anticancer therapy. This indicated that C1orf61 expression benefits HCC patients who are undergoing targeted chemotherapy. Whether C1orf61 contributes to the therapeutic efficacy of other treatments such as radiotherapy or chemotherapeutic agents requires further investigation. Therefore, our data implied that C1orf61 performed diverse functions in liver cancer; many of these underlying features are not yet fully understood. In fact, it genes with known conflicting effects on tumor progression and treatment are very common. Many reports have shown that some proteins that maintain cell homeostasis, such as Akt, mitogen-activated protein kinase (MAPK), NF-κB and p21, directly

contribute to tumor growth and the spread of metastases. [32–34] Such proteins with high activities can sensitize resistant cancer cells to the proapoptotic effects of some anti-cancer agents.

EMT is an important process in which epithelial cells change their phenotype from an apical-basal polarity to a spindle-shaped morphology; epithelial markers (Ecadherin and ccludin) are reduced and mesenchymal markers (N-cadherin, vimentin, and snail) are up-regulated. [35–37] These results in functional changes associated with the conversion of stationary cells to motile cells. In this study, wound-healing and transwell assays showed that cells expressing C1orf61 at high levels exhibited significant EMT potential and migration. Considering that C1orf61 has been described as a potential transcriptional activator that mediates the activation of the human c-Fos promoter, [18] we speculated that EMT in C1orf61-induced liver cancer cells might be the result of the transcriptional regulation of some related genes. Our gene expression profiling analysis further confirmed our hypothesis that C1orf61 regulated the expression of diverse genes and was implicated in cell growth, migration, invasion and EMT (Fig. 2).

One limitation of our study is that we did not obtain transgenic mice despite many attempts. We speculate that C1orf61 plays an essential role in embryo development. To make our data more convincing, we instead performed subcutaneous tumor xenografts and intravenous tumor cell inoculations in athymic nude mice. Both metastasis assays were consistent with our in vitro observations; C1orf61 promoted liver cancer metastasis to the lung and regulated the downstream activation of Akt and STAT3 in vivo. Additionally, our prior gene expression analysis showed that C1orf61 is implicated in embryogenesis during the development of the skeletal system. C1orf61 expression was also found to be associated with low bone mineral density. Approximately 20% of HCC cases involve bone metastasis; [38] whether C1orf61 can promote the metastasis of liver cancer cells to bone is worth exploring, even if it the two issues seem unrelated.

Conclusions

In summary, we demonstrated here that C1orf61 acted as a tumor activator and promoted the metastasis of human hepatocellular cells in vitro and in vivo. Mechanistically, C1orf61 activated the STAT3 and Akt cascade pathways. These pathways induce cellular EMT and result in migration. Meanwhile, C1orf61 improved the therapeutic response to sorafenib in HCC cells. We report here a new regulatory pathway by which C1orf61 facilitates human liver cancer cells metastasis, which increases our understanding of the molecular events that regulate metastasis. C1orf61 may serve an effective candidate for diagnosis, prognosis, and targeted therapy in HCC patients.

Abbreviations

HCC: Hepatocellular carcinoma; EMT; Epithelial-mesenchymal transition; MMPs:Metalloproteinase; TGF-β:Transforming growth factor beta; VEGF:Vascular endothelial growth factor; FGF:Fibroblast growth factor; PDGF:Platelet-derived growth factor; MSCs:Mesenchymal stem cells; ECM:Extracellular matrix;

C1orf61:Chromosome 1 open reading frame 61; STAT3:Signal transducer and activator of transcription 3; HBV:Hepatitis B virus; MAPK:Mitogen-activated protein kinase;

Declarations

Ethics approval and consent to participate

For the animal study, all animal care and experiments were approved by the Experimental Animal Center of Wuhan University.

Consent for publication

All authors agree to submit the article for publication.

Availability of data and materials

All data analyzed during this study are included in this manuscript and its supplementary information files.

Competing interests

The authors declare that they have no competing interests.

Funding

This study was supported by the National Natural Science Foundation of China (81472684).

Author Contributions

Y.Y., Z.W. conducted the experiments; Y.Y., Z.W. created the figures; Z.H., X.T. data collection and analysis. W.L. supervised and designed the research, analyzed and interpreted the data and co-wrote the manuscript.

Acknowledgements

Not applicable

References

1. Awuah PK, Monga SP. Cell cycle-related kinase links androgen receptor and beta-catenin signaling in hepatocellular carcinoma: why are men at a loss? Hepatology. 2012;55:970–3.
2. Forner A, Reig M, Bruix J. Hepatocellular carcinoma. The Lancet. 2018;391:1301–14.
3. Seyfried TN, Huysentruyt LC. On the origin of cancer metastasis. Crit Rev Oncog. 2013;18:43–73.

4. Luna LE, Kwo PY, Roberts LR, Mettler TA, Gansen DN, Andrews JC, Wiseman GA, et al. Liver transplantation after radioembolization in a patient with unresectable HCC. Nat Rev Gastroenterol Hepatol. 2009;6:679–83.
5. Weber GF. Why does cancer therapy lack effective anti-metastasis drugs? Cancer Lett. 2013;328:207–11.
6. Chen J, Chen P, Backman LJ, Zhou Q, Danielson P. Ciliary Neurotrophic Factor Promotes the Migration of Corneal Epithelial Stem/progenitor Cells by Up-regulation of MMPs through the Phosphorylation of Akt. Sci Rep. 2016;6:25870.
7. Clevers H. Wnt/beta-catenin signaling in development and disease. Cell. 2006;127:469–80.
8. Amin R, Mishra L. Liver stem cells and tgf-Beta in hepatic carcinogenesis. Gastrointest Cancer Res. 2008;2:27–30.
9. Poon RT, Ng IO, Lau C, Zhu LX, Yu WC, Lo CM, Fan ST, et al. Serum vascular endothelial growth factor predicts venous invasion in hepatocellular carcinoma: a prospective study. Ann Surg. 2001;233:227–35.
10. Turner N, Grose R. Fibroblast growth factor signalling: from development to cancer. Nat Rev Cancer. 2010;10:116–29.
11. Gialeli C, Nikitovic D, Kletsas D, Theocharis AD, Tzanakakis GN, Karamanos NK. PDGF/PDGFR signaling and targeting in cancer growth and progression: Focus on tumor microenvironment and cancer-associated fibroblasts. Curr Pharm Des. 2014;20:2843–8.
12. Rhim AD, Mirek ET, Aiello NM, Maitra A, Bailey JM, McAllister F, Reichert M, et al. EMT and dissemination precede pancreatic tumor formation. Cell. 2012;148:349–61.
13. Taube JH, Herschkowitz JI, Komurov K, Zhou AY, Gupta S, Yang J, Hartwell K, et al. Core epithelial-to-mesenchymal transition interactome gene-expression signature is associated with claudin-low and metaplastic breast cancer subtypes. Proc Natl Acad Sci U S A. 2010;107:15449–54.
14. Loh CY, Chai JY, Tang TF, Wong WF, Sethi G, Shanmugam MK, Chong PP, et al. The E-Cadherin and N-Cadherin Switch in Epithelial-to-Mesenchymal Transition: Signaling, Therapeutic Implications, and Challenges. Cells 2019;8.
15. Ma L, Hernandez MO, Zhao Y, Mehta M, Tran B, Kelly M, Rae Z, et al. Tumor Cell Biodiversity Drives Microenvironmental Reprogramming in Liver Cancer. Cancer Cell 2019;36:418–30 e416.
16. Spano D, Heck C, De Antonellis P, Christofori G, Zollo M. Molecular networks that regulate cancer metastasis. Semin Cancer Biol. 2012;22:234–49.
17. Vita M, Henriksson M. The Myc oncoprotein as a therapeutic target for human cancer. Semin Cancer Biol. 2006;16:318–30.
18. Jeffrey PL, Capes-Davis A, Dunn JM, Tolhurst O, Seeto G, Hannan AJ, Lin SL. CROC-4: a novel brain specific transcriptional activator of c-fos expressed from proliferation through to maturation of multiple neuronal cell types. Mol Cell Neurosci. 2000;16:185–96.

19. Yi H, Xue L, Guo MX, Ma J, Zeng Y, Wang W, Cai JY, et al. Gene expression atlas for human embryogenesis. FASEB J. 2010;24:3341–50.
20. Mori S, Chang JT, Andrechek ER, Matsumura N, Baba T, Yao G, Kim JW, et al. Anchorage-independent cell growth signature identifies tumors with metastatic potential. Oncogene. 2009;28:2796–805.
21. Thilakasiri PS, Dmello RS, Nero TL, Parker MW, Ernst M, Chand AL. Repurposing of drugs as STAT3 inhibitors for cancer therapy. Seminars in Cancer Biology 2019.
22. Sullivan NJ, Sasser AK, Axel AE, Vesuna F, Raman V, Ramirez N, Oberyszyn TM, et al. Interleukin-6 induces an epithelial-mesenchymal transition phenotype in human breast cancer cells. Oncogene. 2009;28:2940–7.
23. Rojas A, Liu G, Coleman I, Nelson PS, Zhang M, Dash R, Fisher PB, et al. IL-6 promotes prostate tumorigenesis and progression through autocrine cross-activation of IGF-IR. Oncogene. 2011;30:2345–55.
24. Xiong H, Hong J, Du W, Lin YW, Ren LL, Wang YC, Su WY, et al. Roles of STAT3 and ZEB1 proteins in E-cadherin down-regulation and human colorectal cancer epithelial-mesenchymal transition. J Biol Chem. 2012;287:5819–32.
25. Fresno Vara JA, Casado E, de Castro J, Cejas P, Belda-Iniesta C, Gonzalez-Baron M. PI3K/Akt signalling pathway and cancer. Cancer Treat Rev. 2004;30:193–204.
26. Testa JR, Bellacosa A. AKT plays a central role in tumorigenesis. Proc Natl Acad Sci U S A. 2001;98:10983–5.
27. Hara T, Suzuki F, Kawamura Y, Sezaki H, Hosaka T, Akuta N, Kobayashi M, et al. Long-term entecavir therapy results in falls in serum hepatitis B surface antigen levels and seroclearance in nucleos(t)ide-naive chronic hepatitis B patients. J Viral Hepat. 2014;21:802–8.
28. Lai CL, Yuen MF. Prevention of hepatitis B virus-related hepatocellular carcinoma with antiviral therapy. Hepatology. 2013;57:399–408.
29. Liu L, Cao Y, Chen C, Zhang X, McNabola A, Wilkie D, Wilhelm S, et al. Sorafenib blocks the RAF/MEK/ERK pathway, inhibits tumor angiogenesis, and induces tumor cell apoptosis in hepatocellular carcinoma model PLC/PRF/5. Cancer Res. 2006;66:11851–8.
30. Li L, Wang H. Heterogeneity of liver cancer and personalized therapy. Cancer Lett. 2016;379:191–7.
31. Wang C, Vegna S, Jin H, Benedict B, Lieftink C, Ramirez C, de Oliveira RL, et al. Inducing and exploiting vulnerabilities for the treatment of liver cancer. Nature. 2019;574:268–72.
32. Furukawa F, Matsuzaki K, Mori S, Tahashi Y, Yoshida K, Sugano Y, Yamagata H, et al. p38 MAPK mediates fibrogenic signal through Smad3 phosphorylation in rat myofibroblasts. Hepatology. 2003;38:879–89.
33. Tadlock L, Patel T. Involvement of p38 mitogen-activated protein kinase signaling in transformed growth of a cholangiocarcinoma cell line. Hepatology. 2001;33:43–51.
34. Qiao L, McKinstry R, Gupta S, Gilfor D, Windle JJ, Hylemon PB, Grant S, et al. Cyclin kinase inhibitor p21 potentiates bile acid-induced apoptosis in hepatocytes that is dependent on p53. Hepatology.

2002;36:39–48.
35. Choi SS, Diehl AM. Epithelial-to-mesenchymal transitions in the liver. Hepatology. 2009;50:2007–13.
36. Scharl M, Frei P, Frei SM, Biedermann L, Weber A, Rogler G. Epithelial-to-mesenchymal transition in a fistula-associated anal adenocarcinoma in a patient with long-standing Crohn's disease. Eur J Gastroenterol Hepatol. 2014;26:114–8.
37. Tomizawa Y, Wu TT, Wang KK. Epithelial mesenchymal transition and cancer stem cells in esophageal adenocarcinoma originating from Barrett's esophagus. Oncol Lett. 2012;3:1059–63.
38. Berger MF, Levin JZ, Vijayendran K, Sivachenko A, Adiconis X, Maguire J, Johnson LA, et al. Integrative analysis of the melanoma transcriptome. Genome Res. 2010;20:413–27.

Figures

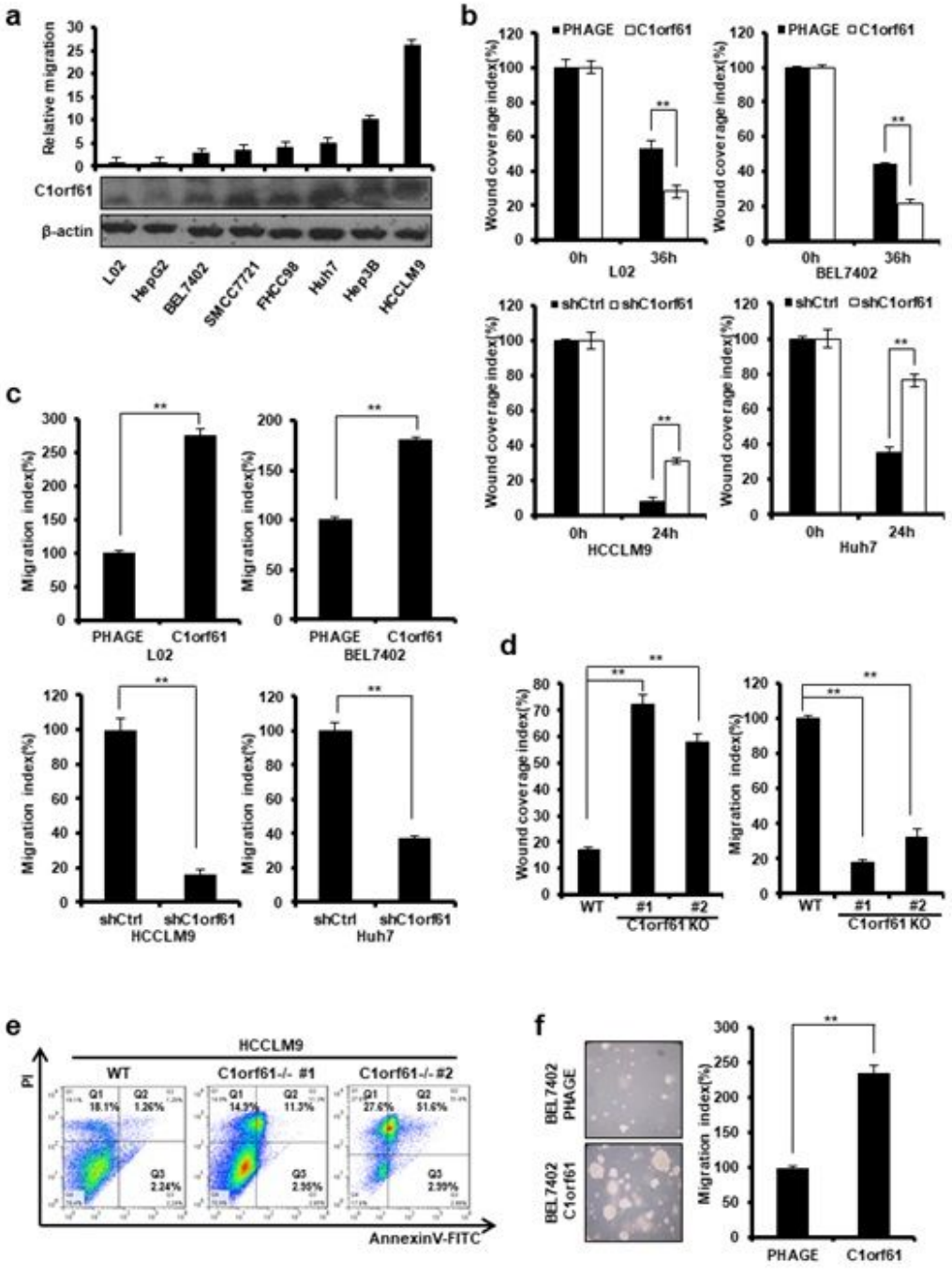

Figure 1

Figure 1

C1orf61 drives migration in human hepatocellular cells. (a) Detection of the migration potential (bars) of indicated hepatocellular cell lines in correlation with endogenous C1orf61 protein levels. C1orf61 was highly expressed in high-migrative hepatocellular cells. Data represent means from at least three independent experiments ±SD. β-actin served as loading control. (b) Cellular migration rates were assessed in HCCLM9, Huh7 cells stably transfected with sh-C1orf61 vector, and BEL7402, L02 cells

stably transfected with C1orf61-overexpressing vector using wound-healing assay. Fold changes were relative to cells transfected with control vector. **P<0.01 by student's t-test. (c) Transwell assay of stable sh-C1orf61 HCCLM9 and Huh7 cells and stable C1orf61-expressing BEL7402 and L02 cells. Migration index was determined by counting cells in 9 randomly selected microscopic fields per well. **P<0.01. (d) Migration possibility were measured in HCCLM9 and HCCLM9 C1orf61-/- cells using wound-healing assay and transwell assay. **P<0.01. (e) HCCLM9 and HCCLM9 C1orf61-/- cells were cultured in suspension condition for 72 h, and then apoptosis was determined by annexinV-FITC/PI for 15 min at room temperature. (f) Left panel: Soft-agar colony formation assay revealed clonogenicity of BEL7402-PHAGE and BEL7402-C1orf61 cells. Right panel: statistical results. BEL7402-C1orf61 expressed higher clonogenicity than BEL7402-PHAGE cells. **P<0.01 by student's t-test.

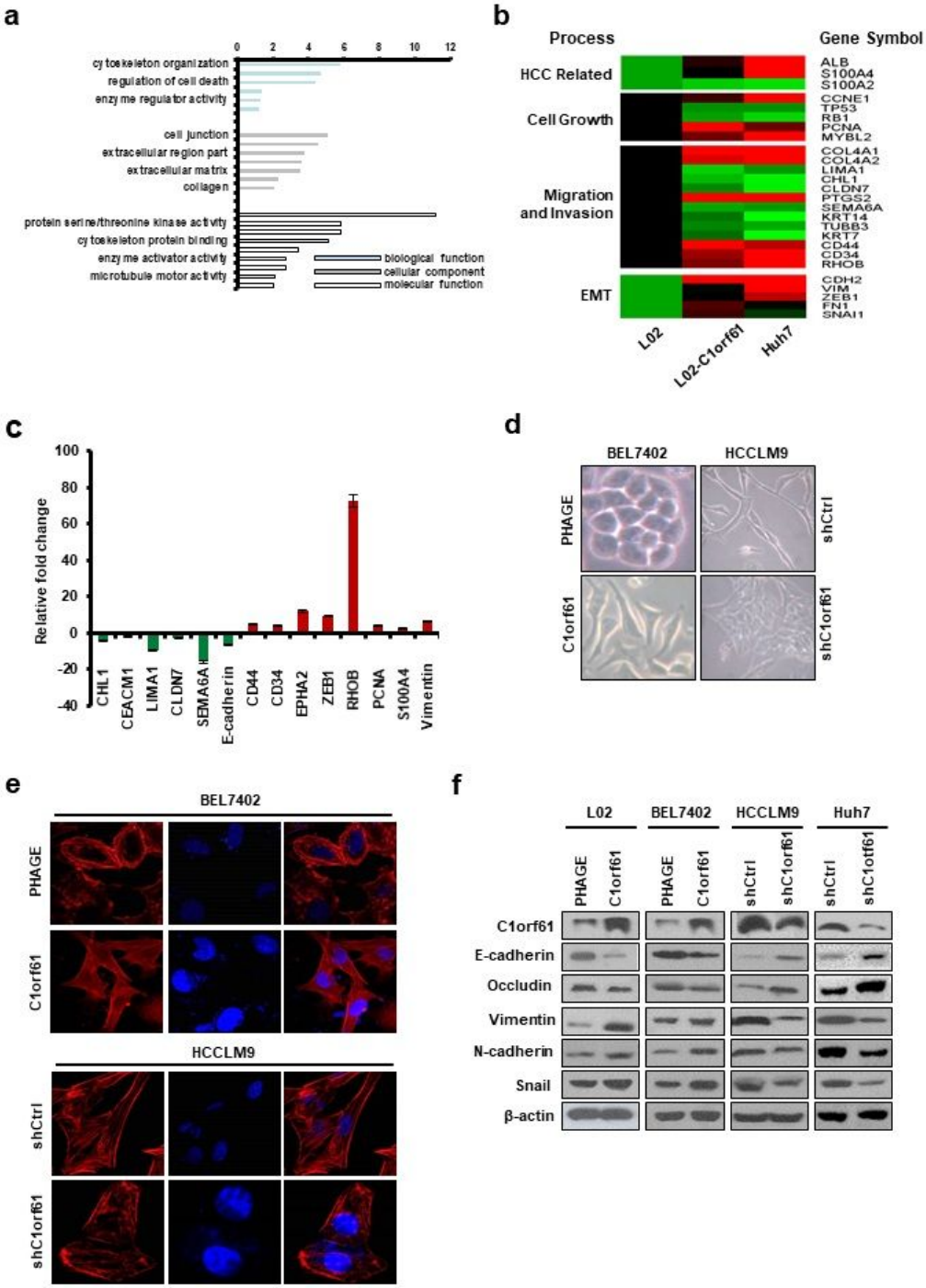

Figure 2

Figure 2

Gene expression patterns associated with cell migration in C1orf61-positive liver cells. (a) Functional annotation clustering of genes regulated by C1orf61 is shown and the enriched groups are named by the gene ontology term of the group member with the most significant p value and are ranked by the groups enrichment scores. (b) Gene expression levels for a subset of genes that are HCC related, cell growth genes, or related to EMT, migration and invasion. Red, high expression; green, low expression. (c) QRT-PCR

of selected genes in L02-C1orf61 vs L02-PHAGE cells. Bar graphs represent mean values of three separate samples measured in triplicate ±SD. (d) Morphology of BEL7402-PHAGE and BEL7402-C1orf61 or HCCLM9 WT and HCCLM9 shC1orf61 cells were determined by phase-contrast microscopy. Overexpression of C1orf61 resulted in a morphological transformation from tightly packed colonies to a spindle-shaped, fibroblastic, dispersed morphology. (e) Stable C1orf61-overexpressing BEL7402 and stable sh-C1orf61 HCCLM9 stained for F-actin (phalloidin, red) and DNA (DAPI, blue) were visualized by confocal fluorescence microscopy compared to BEL7402-PHAGE and HCCLM9-WT cells. Stress fiber and filopodia were detected in HCCLM9 WT and BEL7402-C1orf61 cells, but not in control cells. (f) Expression of EMT markers (E-cadherin, Occludin, Vimentin, N-cadherin and Snail) were assessed by Western blot. β-actin served as a loading control.

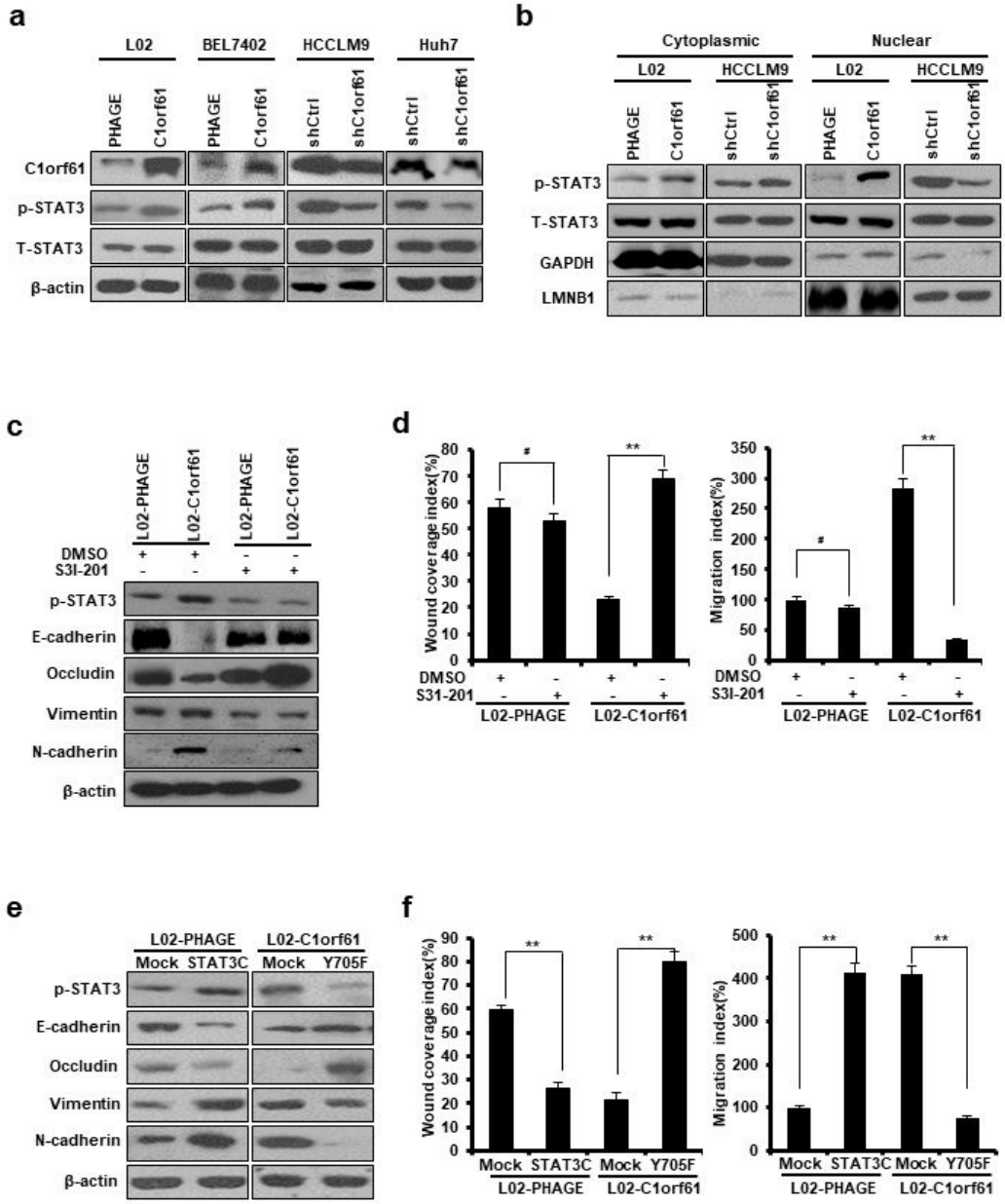

Figure 3

Figure 3

C1orf61 activates STAT3 and STAT3 activity is essential for cellular EMT, migration (a) Western blot analysis was used to analyze the levels of phosphorylated STAT3 (Y705), total STAT3 in BEL7402, L02 cells or HCCLM9, Huh7 cells after C1orf61-overexpression or knockdown of C1orf61 in compared to controls. β-actin served as a loading control. (b) Detection of p-STAT3 (Y705) in the nuclear and cytosolic fraction of L02-PHAGE, L02-C1orf61 and HCCLM9-shCtrl, HCCLM9-shC1orf61 cells. GAPDH and LMNB1

were used for equal loading. (c) L02-PHAGE and L02-C1orf61 cells were treated with 50 μM S3I-201 (NSC74859) for 48 hr, expression of EMT markers were detected by Western blot. β-actin served as a loading control. (d) Wound healing assay and transwell assay were used to explore the influence of S3I-201 on cellular migration. They revealed that the migration index of L02-C1orf61 cell were significantly lower after treated with 50 μM S3I-201. **P<0.01. (e) Significant decreases in epithelial gene (E-cadherin, Occludin) and increases in the mesenchymal gene (Vimentin, N-cadherin) were found in L02-PHAGE cells transfected with STAT3C by Western blot, vice versa in L02-C1orf61 cells transfected with STAT3 Y705F. β-actin served as a loading control. (f) Wound healing assay and transwell assay revealed that constitutively activate p-STAT3 would induce cell migration, whereas inhibition of p-STAT3 activation would reduce cell migration. **P<0.01.

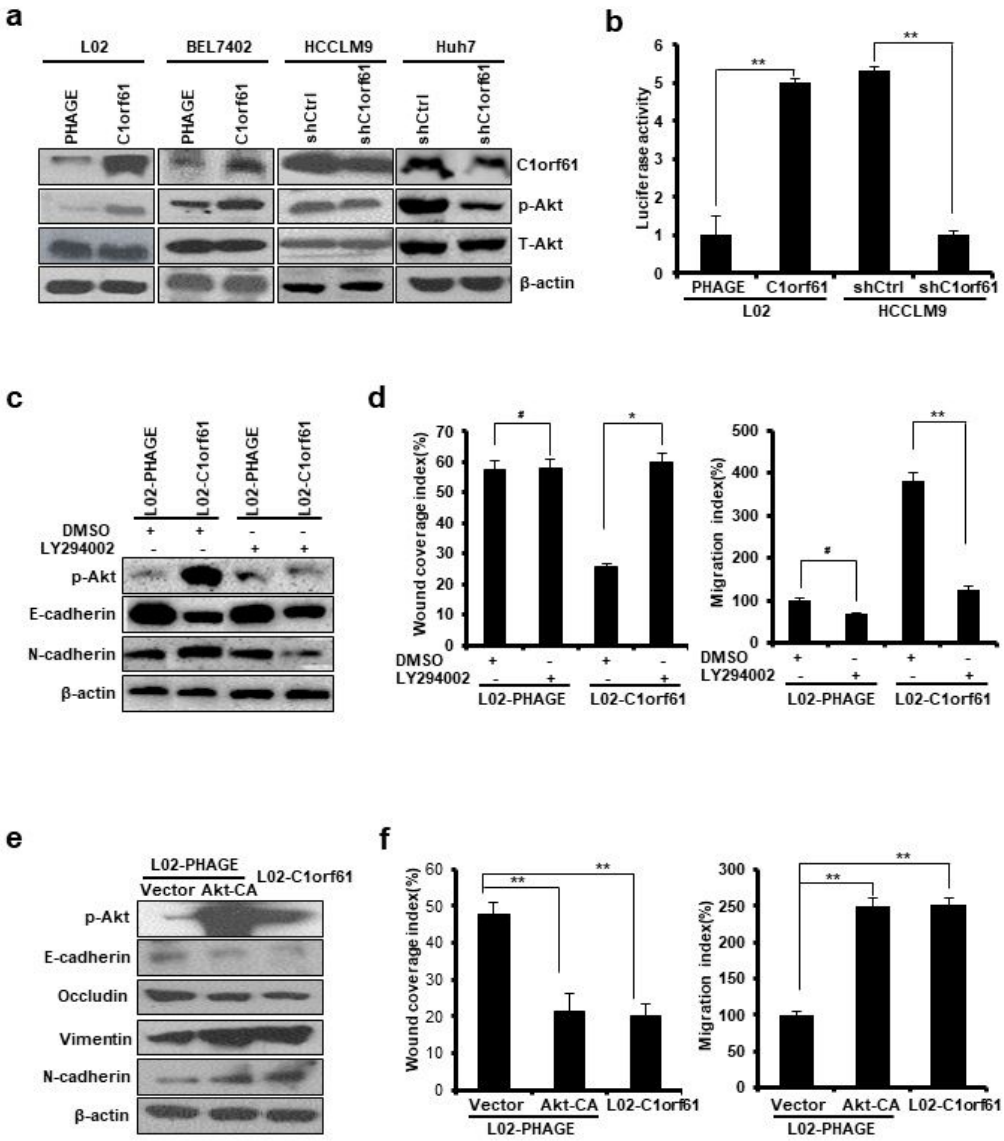

Figure 4

Figure 4

P-AKT is also involved in C1orf61-induced cell migration (a) Levels of p-Akt (S473) in BEL7402, L02 or HCCLM9, Huh7 cells compared to C1orf61-overexpression or shC1orf61 cells by Western blot. β-actin served as a loading control. (b) Akt luciferase activities (RLU) were shown 36 h after transfection in L02-C1orf61 and HCCLM9- shC1orf61 cells relative to L02-PHAGE and HCCLM9-shCtrl scrambled control cells. Error bars indicate one SD of the mean from three separate experiments. **P<0.01 by student's t-

test. (c) L02-PHAGE and L02-C1orf61 cells were treated with 10 μM LY294002 for 48 h, expression of EMT markers were detected by Western blot. β-actin served as a loading control. (d) Wound healing assay and transwell assay revealed that cellular migration was inhibited while L02-C1orf61 cells were treated with 10 μM LY294002. **P<0.01. (e) L02-PHAGE cells were transfected with either vehicle or constitutively active Akt (Akt CA), and then expression of EMT markers were detected by Western blot. L02-C1orf61 cells acted as a positive control. β-actin was used as a loading control. (f) Cellular migration rates were determined in the L02-PHAGE cells transfected with either vehicle or CA-Akt by wound healing assay and transwell assay. L02-C1orf61 cells acted as a positive control. *P<0.05, **P<0.01.

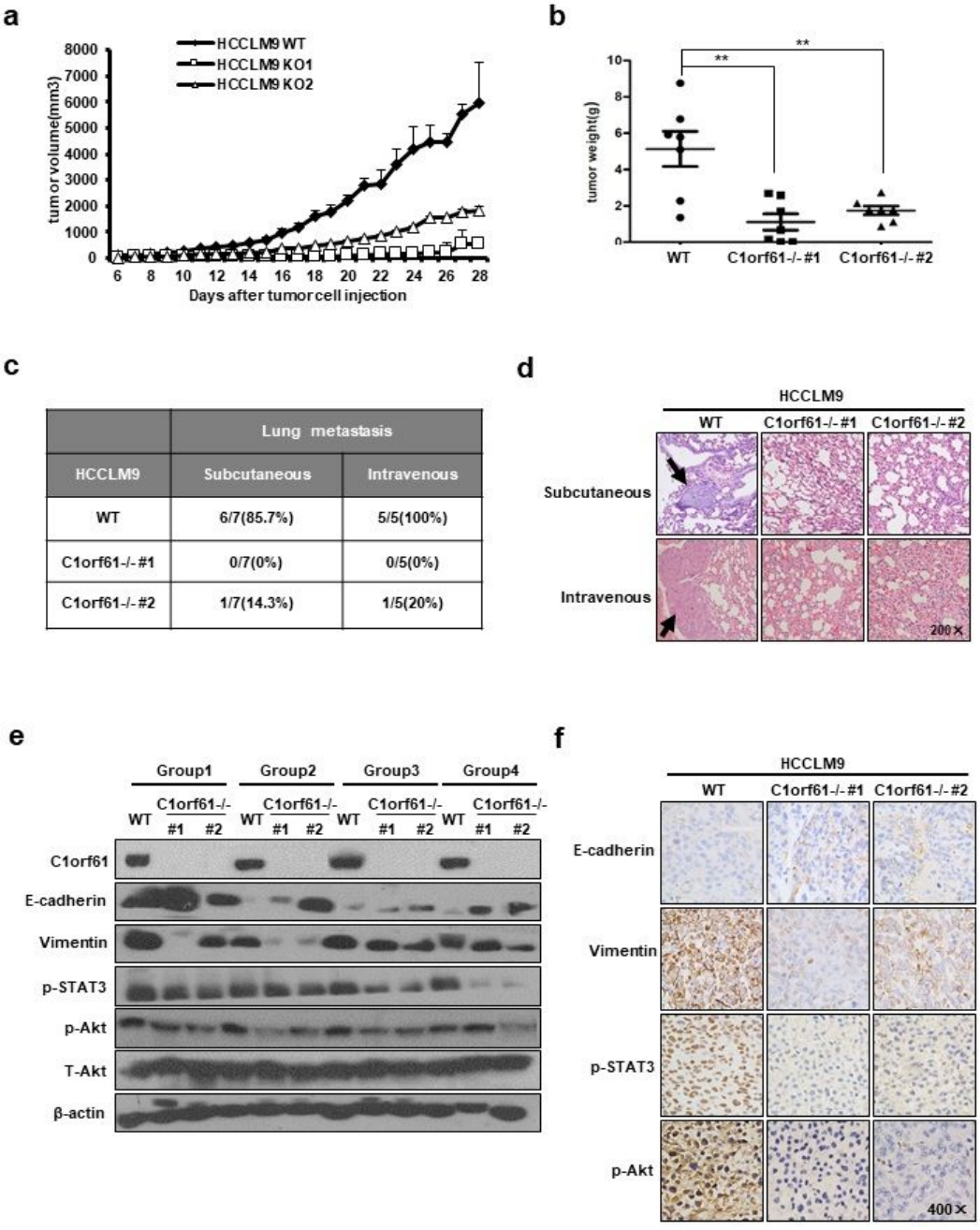

Figure 5

Figure 5

C1orf61 promote tumor growth and metastasis in vivo (a) HCCLM9 and HCCLM9 C1orf61-/- cells were inoculated into BALB/C mice to establish a tumor model as indicated in the materials and methods. Tumor volumes were measured daily. (b) Tumors were extracted and weighed after 28 days of tumor cell injection, and the data are presented as a scatter plot; the bars represent the SD. **P<0.01. (c) Lung metastasis capacity of s.c and vein intravenous injection xenograft with and without C1orf61 expression.

(d) Representative lungs H&E sections from mice carrying tumors of HCCLM9 WT and HCCLM9 C1orf61-/- cells via s.c.injection (top) and tail intravenous injection (bellow). Arrows indicate lung metastases. Magnification: ×200. (e) Tumor tissues were isolated from HCCLM9 WT and HCCLM9 C1orf61-/- cell xenografts and EMT makers (E-cadherin, Vimentin), phosphorylate STAT3 and phosphorylate Akt, total Akt were determined by Western blot. 3 mice in each group have been defined as WT, “#1” and “#2”, respectively. β-actin was used as a loading control. (f) Immunohistochemistry of tumor tissues from HCCLM9 WT and HCCLM9 C1orf61-/- cell xenografts. Sections were stained with antibodies against E-cadherin, Vimentin, p-STAT3, and p-Akt/Akt. Magnification: ×400.

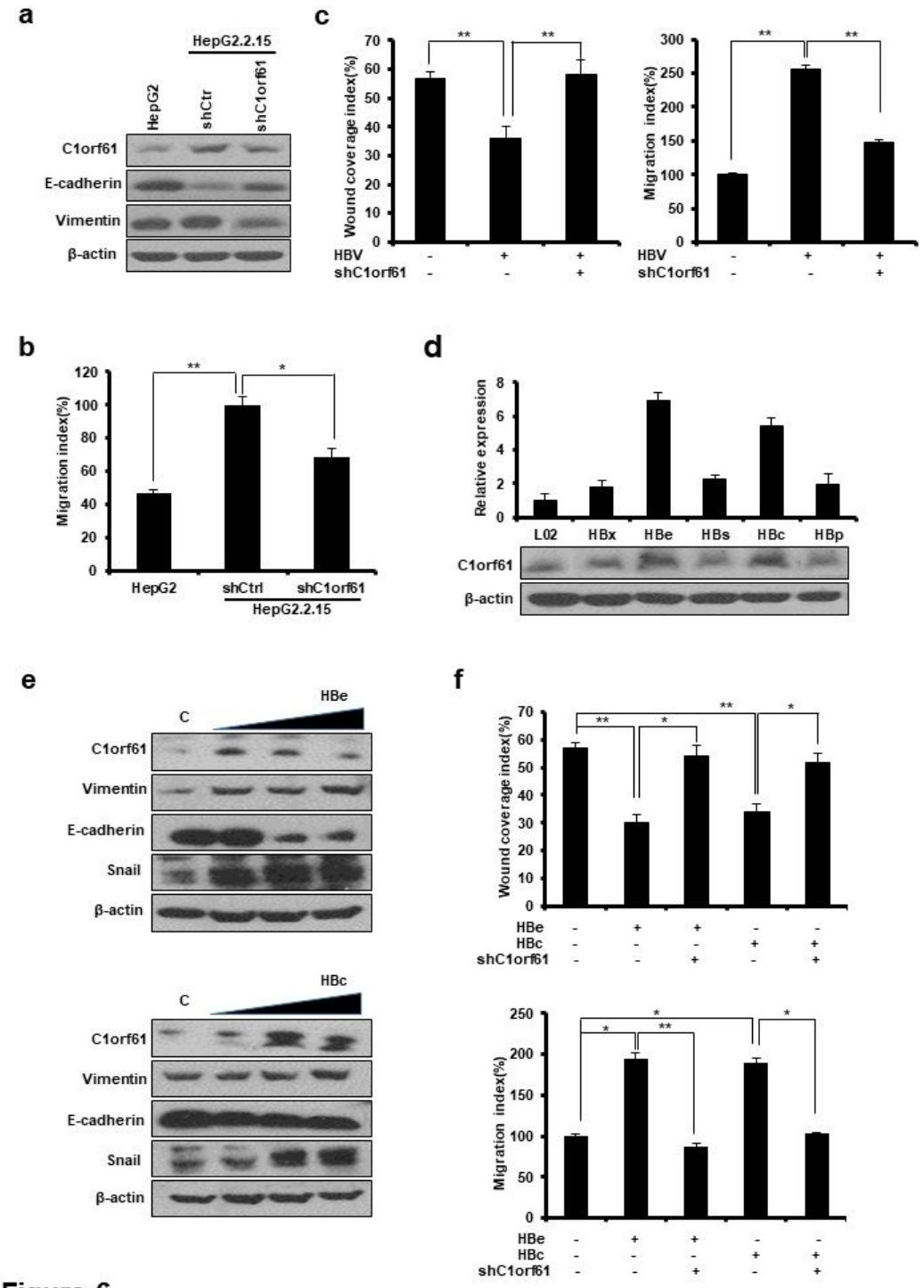

Figure 6

Figure 6

C1orf61 expression is induced by HBV infection and is related to HBe and HBc (a) Western blot analysis was used to detect the endogenous C1orf61 expression in HepG2 and HepG2.2.15 cells, and the expression of EMT markers (E-cadherin, Vimentin). β-actin was used as a loading control. (b) Cellular migration capacity was measured after HepG2.2.15 cells were transfected with shC1orf61 vector by transwell assay. *P<0.05, **P<0.01. (c) Wound-healing assay and transwell assay were used to detect the

cellular migration index after L02-PHAGE cells were transfected with HBV vector, and cotransfected with HBV and shC1orf61 vector. Fold changes were relative to HepG2 cells. *P<0.05, **P<0.01. (d) QRT-PCR and Western blot analysis were used to explore the elements that related to C1orf61 induced cell migration. Transient expression of HBe and HBc remarkably increased mRNA and protein level of C1orf61. β-actin was used as a loading control. (e) L02-PHAGE cells were transfected with increasing amounts of HBe or HBc expression vector (0, 1, 2, 4 μg), C1orf61 expression level and EMT markers were detected by western blot analysis. β-actin was used as a loading control. (f) L02-PHAGE cells were transfected with HBe, HBc expression vector, or cotransfected with HBe, shC1orf61 or HBc, shC1orf61 expression vector. Cellular migration capacity was assessed by wound-healing assay and transwell assay. *P<0.05, **P<0.01.

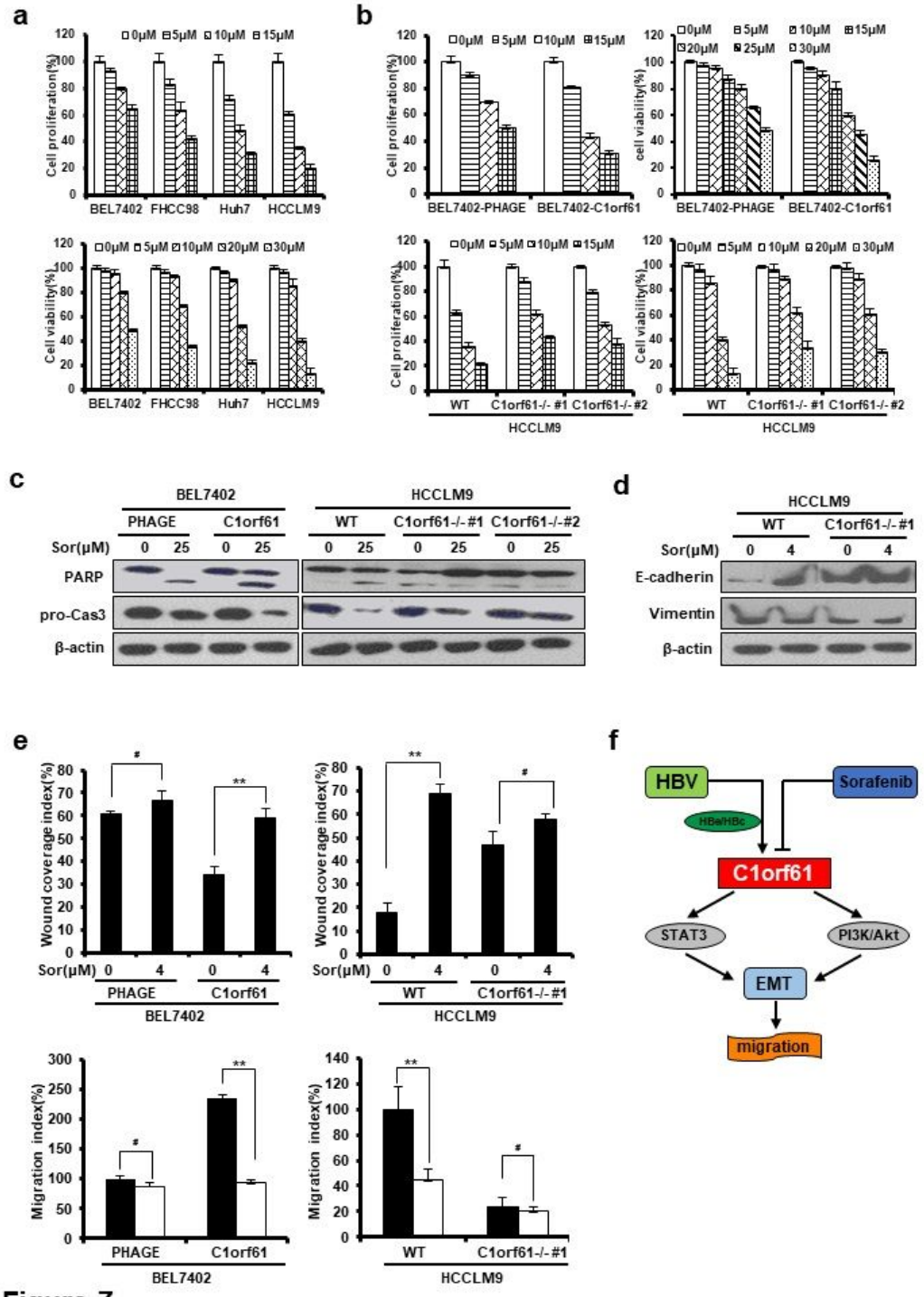

Figure 7

Figure 7

Sorafenib efficiently induces cell apoptotic cell death in C1orf61-positive hepatocellular carcinoma cells (a) BEL7402, FHCC98, Huh7 and HCCLM9 cell lines were treated with 0 (DMSO), 5, 10, 15, 20, 30 μM sorafenib for 48 h, cell proliferation and cell viability were assessed by trypan blue exclusion assay. (b) Cellular proliferation and cell viability were assessed in BEL7402-PHAGE, BEL7402-C1orf61 cells and HCCLM9 WT, HCCLM9 C1orf61-/- cells after treated with 0 (DMSO), 5, 10, 15, 20, 25,30 μM sorafenib for

48 hr. (c) Western blot analysis to detect apoptosis-related PARP, caspase 3 proteins in cells treated with 25μM sorafenib for 48 hr. β-actin was used as a loading control. (d) EMT markers (E-cadherin, Vimentin) were assessed by western blot analysis after cells were treated with 4 μM sorafenib for 48 hr. β-actin was used as a loading control. (e) Cellular migration index was determined in BEL7402-PHAGE, BEL7402-C1orf61 cells and HCCLM9 WT, HCCLM9 C1orf61-/- cells after treated with 4 μM sorafenib by wound-healing assay and transwell assay. (f) Model of C1orf61-induced hepatocellular carcinoma cells migration.

Supplementary Files

This is a list of supplementary files associated with this preprint. Click to download.

- supplementfigure.docx